Applied Decision Analytics

Journal homepage: www.ada-journal.org
ISSN: XXXX-XXXX

Evolution of Holocene Floodplain of Jaldhaka River in Cooch Behar Plain of West Bengal, India

Mantu Das[1,*], Dr. Snehasish Saha[2]

[1] Research Scholar, Department of Geography & Applied Geography, University of North Bengal, Darjeeling, West Bengal, India
[2] Associate Professor, Department of Geography & Applied Geography, University of North Bengal, Darjeeling, West Bengal, India

ARTICLE INFO

Article history:
Received 25 June 2025
Received in revised form 15 September 2025
Accepted 9 October 2025
Available online 11 November 2025

Keywords:
Holocene, Floodplain, Himalayan foreland basin (HFB), Jaldhaka River, Fluvial processes

ABSTRACT

This study evaluates how the river networks and floodplain geomorphology of the Jaldhaka River have changed within a dynamic Himalayan foreland basin environment over an 88-year period (1934–2022). Floodplain geomorphological maps were prepared using high-resolution satellite images and historical maps. Field validation contributed to improving the accuracy of landform mapping, while sedimentary log analysis allowed the recognition of floodplain types and fluvial architectural elements. Channel oscillation attributes were interpreted based on indices such as channel length, channel width, and sinuosity, as well as bankline migration and erosion–accretion areas. The findings suggest that progressive channel migration and meander shifting have shaped various floodplain landforms in the recent past, such as cut-offs, palaeochannels, backswamps, abandoned channels, and meander scroll bars on a Holocene river plain. These features are well developed in the middle and lower floodplains. Quantitative analysis indicated that the channel sinuosity of the middle and lower segments of the Jaldhaka River fluctuated (1.15, 1.24, 1.42, 1.18, and 1.31 for the years 1934, 1955, 1983, 2003, and 2023, respectively), implying channel lengthening or shortening due to meander development and cut-off formation processes taking place over time. The results also demonstrate spatiotemporal variations in channel width and an increasing trend in erosion–accretion areas during the period 1983–2023. Both natural processes (such as variable discharge, frequent flooding, active tectonics, meander migration, and channel shifting) and human interventions (including channelization, mining, construction of cross-sectional structures, and land-use changes) have contributed to the evolution and morphological modification of the Jaldhaka River system and its floodplains in the Cooch Behar Plain, West Bengal.

1. Introduction

A key component of an alluvial river system is the floodplain. On either side of the river, there is fertile land, and civilizations have long developed in the floodplains of significant rivers. Floodplain is defined as the comparatively flat area surrounding the active river channel that floods during heavy flow events [1]. Fluvio-hydrological processes play a large role in the evolution and development of

* *Corresponding author.*
E-mail address: rs_mantudas@nbu.ac.in

https://doi.org/10.66972/ada2120268

floodplains. According to Nanson and Croke [2], the three main processes are braid-channel accretion, overbank vertical accretion, and lateral point bar accretion in the floodplain. The accretion of coarser sand and gravel is a characteristic of lateral point bar accretion. Although, according to Wolman and Leopold [3], fine silt and clay depositions may aid in the formation of point bars. On the other hand, silt and clay deposition make up the majority of overbank vertical depositions [3]. For the formation and evolution of floodplains, there are many different types of deposition aside from lateral and vertical depositions, such as channel fill deposition, channel lag deposition, and colluviums [4].

Nanson and Croke [2] distinguished three main types of floodplains based on specific stream power per unit width at bank-full stage and sediment texture: (i) confined coarse textured floodplains with high energy; (ii) non-cohesive floodplains at meandering and braided course with medium energy; and (iii) cohesive floodplains at low energy. The upper and middle reaches of the river, where a small, limited valley prevents lateral channel migration, are where constrained coarse textured floodplains are most commonly seen. The lateral accretion of point bars and braided channel may be regarded as the primary process of floodplain creation and evolution in the case of non-cohesive floodplains along meandering and braided courses. By the accumulation of finer materials, cohesive floodplains can form in anastomosing or single-thread channels [2]. To manage a floodplain or a river, it has been found to be important to comprehend the morphology of the floodplain and how it changes over time [5]. According to Segura-Beltran and Sanchis-Ibor [6], continual channel adjustment allows the floodplain to change over time in response to changes in the discharge and sediments that enter the channel. As a result, various geomorphic features of the floodplain, including levees, crevasse splays, meander scroll bars, cut-offs, palaeochannels, spill channels, abandoned channels, backswamps, etc., may occur. These floodplain landforms are crucial to the fluvial system because they can document the evolutionary history of river floodplains [7]. The drainage, sediment movement, and maintenance of the main channel's link all depend on floodplain channels [8, 9]. Paleochannels can be used to reconstruct the history of channel migration [10] and investigate palaeoclimatic changes [11]. Cut-offs result in an oxbow lake, which reduces the length of the channel and produces topographic diversity and a sediment sink within the floodplain [12]. Thus, cut-offs regulate the sedimentary systems of river floodplains and have an impact on the morphodynamics of rivers [13, 14]. Furthermore, the river and floodplain aquatic ecosystem's habitat diversity is enhanced by oxbow lakes and cut-offs [15, 16]. Furthermore, floodplains act as historical archives that facilitate the reconstruction of the river evolution history of a particular region [5]. Consequently, a thorough grasp of the development of floodplain and river networks, as well as the identification of diverse floodplain geomorphic features, are crucial for a sustainable river management strategy. However, floodplain geomorphic features in most river systems around the world have changed recently due to climatic [17] and human-induced [5, 18] changes [19]. Additionally, floodplains in most river systems worldwide have undergone significant changes due to LULC changes [20].

One of the world's biggest and most active collision basins is the Himalayan foreland basin. A depression was created in front of the Himalayan Orogen as a result of the Indian plate bending from the Eurasian plate's crustal stress. Sediment from the Himalayan mountain belt was used to fill this depression and create a sedimentary foreland basin. Actually, according to Chakraborty et al. [21], the study region is located beneath foredeep depozones of the eastern Himalayan foreland basin system. The Main Frontal Thrust (MFT), which is located south of the Sub-Himalaya and separates it from the current foreland basin, is responsible for this division [22]. Himalayan tectonics, climate, and river accretion all have an impact on the foreland basin's sedimentation process and structural makeup. The spatiotemporal configuration of channel behavior, channel bed, and floodplain

deposition are consequently impacted [23]. Since the rivers in the Himalayan foreland plain flow via a dynamic transition zone between a hilly area and the foreland plain, this causes channel shifting, channel migration, and avulsion. The development of a spill channel in this zone is primarily regulated by the abrupt drop of channel gradient in the piedmont and foothills areas. Cut-offs, palaeochannels, abandoned channels, meander scroll bars, and backswamps are just a few of the floodplain geomorphic features that the river Jaldhaka has created on its floodplain over the course of geological time. These features serve as fluvial archives that record the development and alteration of river floodplains. Prior until this, a small number of scholars have looked into many facets of fluvial geomorphology in the Himalayan foreland basin, but no one had looked into the identification and mapping of floodplain geomorphological features and their evolution, especially in the Jaldhaka river system. Therefore, the primary goals of the current study are to (i) identify floodplain geomorphological features and old river courses on floodplain surfaces, (ii) present the fluvial systems and floodplain landforms through geomorphic mapping, and (iii) investigate the factors that influence the evolution of river networks and floodplain landforms over the recent past (1935-2023). For learning more about water bodies, palaeochannels, sedimentology, and the geomorphology of river floodplains, remote sensing techniques are highly helpful. Due to the benefits of multi-temporal satellite pictures, identification and mapping of floodplain geomorphological features have become simpler with the development of remote sensing and GIS techniques [24]. In order to identify and map floodplain geomorphological features and their evolution, the current study used geospatial techniques and a field-based approach based on sedimentary log analysis.

2. Geographical Account of the Study Area

The Jaldhaka River originates from Bitang Lake in Sikkim at an elevation of about 4,400 m. Flowing through Sikkim, Bhutan, West Bengal, and Bangladesh, the river receives numerous tributaries in both mountainous and sub-mountainous regions before flowing southwestward (S–W) to join the Dharala River. The combined Jaldhaka–Dharala system ultimately discharges into the Brahmaputra River in Bangladesh [25, 26, 27, 28]. The Jaldhaka River has a total length of about 192 km, of which 122 km lies within Indian Territory. Its catchment area covers approximately 5,920 km², with about 3,950 km² located in India (Figure 1). The river has a massive catchment area and is greatly cut into the Dooars area and it moves through the out and out blocks of the tectonics which are actively raising and causing a surface of fan towards the later part of the course [29].

The Jaldhaka River Basin is located in the extreme northeastern part of West Bengal, where the river serves as a riverine international boundary between Bhutan and India. It forms a mid-interfluvial basin positioned between two major river systems of the Brahmaputra Basin—the Teesta to the east and the Torsa to the west. Geologically, the basin exhibits clear imprints of neotectonic activity. According to Geological Survey of India (GSI) reports, the Jaldhaka River Basin comprises twelve distinct lithological formations: Kanchenjunga Gneiss (Proterozoic), Baikunthapur (Pleistocene–Holocene), Chungthang (Proterozoic), Kamarchinwa (Pliocene–Pleistocene), Damuda (Permian), Reyang (Proterozoic), Gorubathan (Proterozoic), Duars (Pleistocene), Buxa (Proterozoic), Jalpaiguri (Holocene), Shaugaon (Holocene), and present-day deposits (Meghalayan). These formations are members of the Matiali, Chalsa, and Samsing groups. The basin exhibits numerous floodplain features—such as cut-offs, palaeochannels, spill channels, natural levees—and channel-bed geomorphic elements including mid-channel bars, islands, and shoals, all of which preserve the history of fluvio-hydrological landscape evolution.

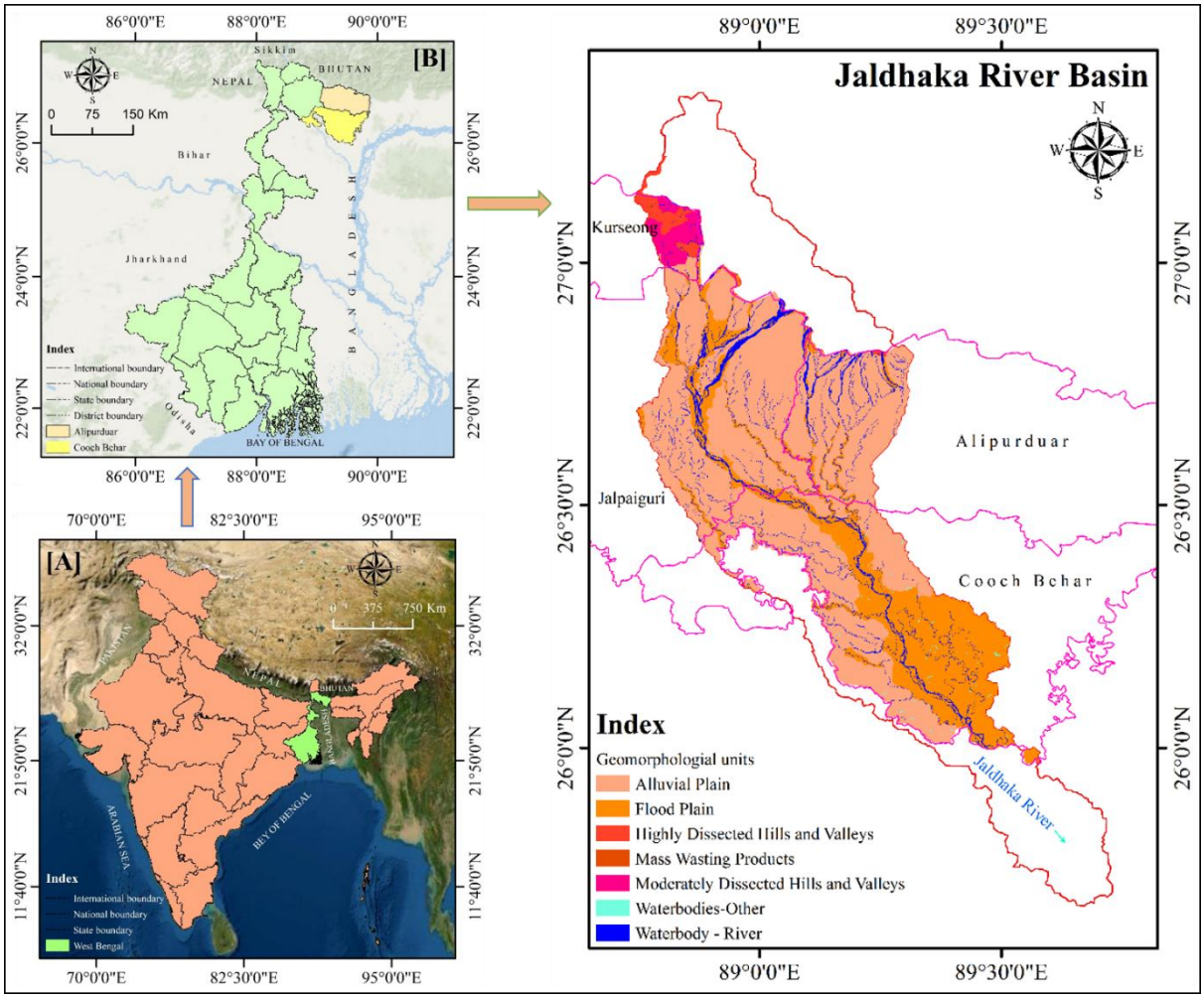

Fig. 1. Locational identity of the study area. Sand, silt, and clay composed newer alluvium, under the Shaugaon formation (present day deposit) of Holocene epoch starting from 0.0117 Ma to present day, is the dominant surface feature created by fluviogenic processes

3. Database and Methodology

3.1 Data Acquisition

Historical data on the drainage network of the Jaldhaka River system were obtained using satellite imagery and old maps, particularly to identify former river courses, cut-offs, meander scroll bars, and backswamps within the study area. The U.S. Army Corps of Engineers Series-U502 map (1955; scale 1:250,000) was accessed via the Army Map Service (RMBM). on the U.S. Army Corps of Engineers website (http://maps.lib.utexas.edu). Landsat 1–3 MSS satellite images of 1972 and 1979 (Path: 148, Row: 42, Spatial Resolution: 60 m), Landsat 4–5 MSS/TM satellite image of 1987 (Path: 138, Row: 42, Spatial Resolution: 30 m) and Landsat 8 OLI/TIRS satellite image of 2020 (Path: 138, Row: 42, Spatial Resolution: 30 m) were collected from USGS website (http://earthexplorer.usgs.gov/). Spatial data on the geology, geomorphology, and hydrogeology of the study area were obtained from the hydrogeological maps of Alipurduar and Cooch Behar, as well as the district resource map of Cooch Behar. Shuttle Radar Topography Mission (SRTM) data (acquired on 10 April 2016, with a spatial resolution of 30 m) were retrieved from the USGS website (http://earthexplorer.usgs.gov/) for generating elevation profiles of the study area. Initially, a layer stack of all satellite images was created using ERDAS Imagine 2014. Geometric and radiometric corrections were then applied

following the methodology of Mujabar and Chandrasekar [30]. Subsequently, the images were re-projected to the UTM system (Northern Hemisphere, Zone 45) using the WGS 84 datum to enhance spatial accuracy in ArcGIS 10.8. The U.S. Army Corps of Engineers Series-U502 maps (1955) were also geo-referenced in ArcGIS 10.8, achieving a root mean square error (RMSE) of less than 0.005 per pixel. To standardize all images to a 30 m resolution, the nearest neighbor interpolation technique was employed. During geometric correction, an image-to-image registration technique was applied. Additionally, re-registration was performed using several recognizable street junctions to ensure consistent geographic alignment across all images. Following re-registration, vector data were generated from the raster datasets in ArcGIS to enable measurements of channel length, channel width, sinuosity, and bank line shifts.

3.2 Hydrological Data

To examine the hydraulic impacts upon formation and evolution of floodplain geomorphological features, the discharge data of two stations i.e., Jaldhaka Barrage at Bindu (monthly discharge data from 1993 to 2005) and Jaldhaka Bridge at NH-31 crossing (annual discharge data from 1978 to 2018) has been used. Various secondary data regarding gauge height during flood season (2013 to 2021) and floods scenarios in the study area is collected from the annual flood report of Government of West Bengal, India (https://wbiwd.gov.in/index.php/applications/anual_flood_report).

3.3 Geospatial Techniques

3.3.1 Geomorphological mapping of floodplain

For the present study, 88 years of time span (1934–2023) has been considered. The old map of 1934 and 1955 (Topographical maps) are used for detailed mapping of river Jaldhaka floodplain in Cooch Behar. Besides, satellite images of the years 1973, 1993, 2003, 2013 and 2023 have also been used for geomorphological mapping of the study area. Watercourses, including the main river, tributaries, and distributaries, were extracted using the MNDWI method, as described in the following sub-section. Following extraction, the outermost boundaries were manually digitized as riverbank lines according to the methodology of Rhoades *et al*. 2009. Each geomorphological feature—such as palaeochannels, cut-offs, abandoned channels, backswamps, meander scroll bars, and channel bars—was then digitized as lines or polygons in ArcGIS 10.8 to delineate their boundaries. Distinct colors and hatching styles were applied to accurately represent individual landforms on the maps. Finally, a comprehensive GIS database was created for subsequent analysis.

3.3.2 Modified Normalized Difference Water Index (MNDWI)

Initially, multi-spectral satellite imagery for the years 1973, 1993, 2003, 2013 and 2023 have been re-sampled and rectified in Erdas Imagine 2014 software. In this context, two steps have been performed. Firstly, the pixel value of the green band and the near infrared band has been converted to the surface reflectance value to clearly extract the object. At first, DNs value of the band (green and near infrared band) was converted to the ToA radiance by the spectral radiance scaling method and ultimately converted to the ToA reflectance. Second, the required atmospheric correction has been performed in the GIS environment [31, 32, 33]. And finally the rectified multi-spectral bands are used to make the NDWI.

The NDWI is the most acceptable technique of identification of the water content on earth surface from satellite imagery. It's a band ratio approach that is generated from a number of band

combinations. This approach is used to differentiate between water body and land features on the surface of the earth by analysing the spectral signatures of each element. NDWI has been determined using the following equation [34, 35]

$$\text{NDWI} = \frac{(\text{Green band} - \text{SWIR band})}{(\text{Green band} + \text{SWIR band})}$$ (modified according to [35])

Four multi-spectral satellite data is used to assess and delineate the changing nature of the river course in temporal perspective over the physical settings. Through this model the researcher can easily extract the stream channel. Noticeable is that the positive value of NDWI implies the water body on the surface of the earth, while the negative value represents the dry land or other components.

3.3.3 Assessment of channel oscillation

Remote sensing and GIS have been used to undertake morphometric analysis. Some indices i.e. Sinuosity Index [36, 37], Braided Index [38], Meander-bend curvature [39] etc. have been applied in geomorphological study to access the spatio-temporal changes of river course with proper mathematical equations.

$$\text{Hydraulic sinuosity index (HSI)} = \frac{(\text{Channel index} - \text{Valley index})}{(\text{Channel index} - 1)}$$ [40]

$$\text{Topographic sinuosity index (TSI)} = \frac{(\text{Valley index} - 1)}{(\text{Channel index} - 1)}$$ [40]

$$\text{Standard sinuosity index (SSI)} = \frac{\text{Channel Index}}{\text{Valley Index}}$$ [40]

$$\text{Braided index (BI)} = \frac{2\ (\text{sum of length of islands or bars})}{\text{Total length of the reach}}$$ [24]

4. Results

4.1 Geomorphological Settings of the Floodplain Using Vintage Maps from 1934 to 2023

The Coochbehar Plain represents an active foreland basin developed in response to Himalayan uplift and associated sediment influx. The stratigraphic succession shows a transition from Older Alluvium (Baikunthapur Formation) of Pleistocene–Holocene age to Newer Alluvium deposits of Holocene–Meghalayan age. The Baikunthapur Formation's calcareous concretions indicate alternating wet and dry climatic conditions and prolonged subaerial exposure. In contrast, the Shaugaon and Jalpaiguri formations reflect fluvial reworking under dynamic river systems during the Holocene. Feeble oxidation in the Jalpaiguri Formation suggests limited pedogenesis and fluctuating water tables. The current deposits show continuous sedimentation beneath rivers that are fed by the Himalayas. This vertical transition from oxidised to fresh alluvium shows how ongoing Himalayan tectonism has rejuvenated river systems. Deposition in a low-gradient alluvial plain is reflected in the general lithologic homogeneity of sand, silt, and clay. The interaction of tectonics, climate, and riverine processes that shaped the Himalayan foreland landscape over time is thus preserved in the Coochbehar Plain.

The two thematic maps in Figure 2 show the geomorphology (a) and lithology (b) of the Cooch Behar Plain. Together, they show how important fluvial processes are in shaping and changing the landscape.

Map (a) shows that the geomorphological features show a landscape that has been strongly shaped by the way rivers move and sediment settles. Active and younger alluvial plains cover most

of the area. This shows that river channels are constantly depositing sediment. The presence of meander scars, oxbow lakes, abandoned channels, and cut-off meanders clearly indicates active lateral channel migration, which is a common feature of a mature meandering river system. Natural levees and braid bars along the main channel zones suggest that the water sometimes floods over the banks and moves sediment around. Channel Islands and bars are places where sediment settles in the middle of the channel. Dissected alluvial fans are places where the energy of the river decreases, which causes sediment to spread. The wide floodplain systems, both new and old, show that there has been a lot of channel avulsion, aggradation, and floodplain reworking over a long time. Marshes and water bodies such as ponds and oxbow lakes occupy the low-lying, poorly drained areas, signifying the later stages of channel abandonment.

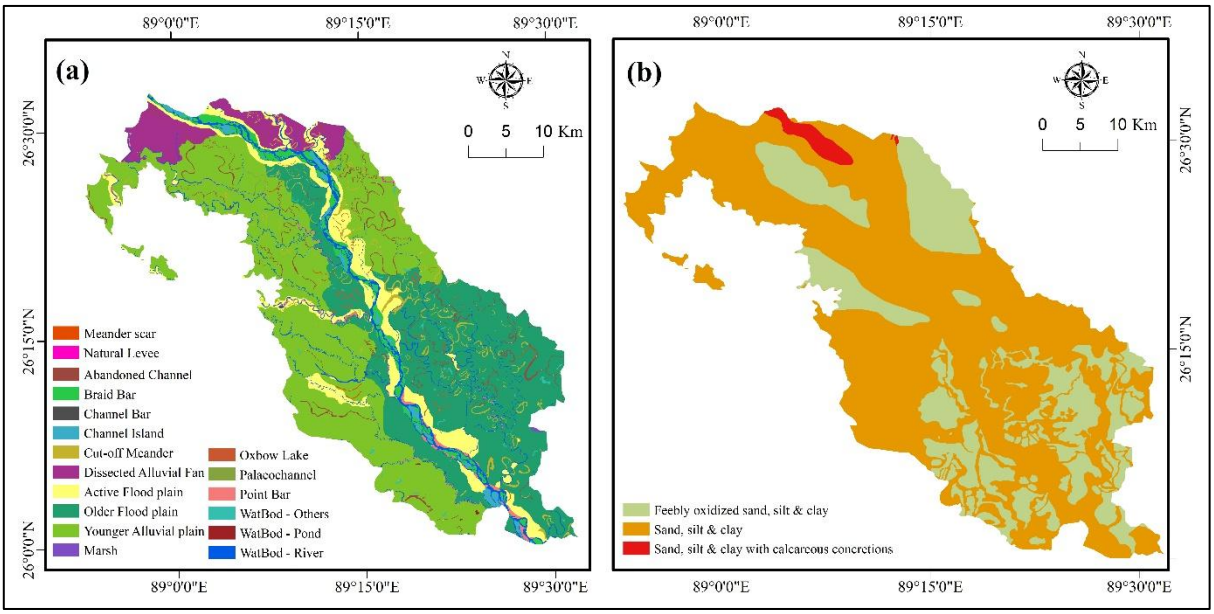

Fig. 2. Physical settings of the Jaldhaka River Basin in Cooch Behar plain (a) Geomorphology (b) Lithology

In map (b), the lithological composition closely matches the geomorphic features and the way the rivers flow. The fact that there is a lot of sand, silt, and clay means that there are fluvio-alluvial deposits that were made by different flow regimes. For example, coarser sands are found along channels and finer silts and clays are found on the floodplains. The weakly oxidised sand, silt, and clay areas show that sedimentation is happening in sub-humid, low-oxygen conditions that are common in floodplain environments. The patches of sand, silt, and clay with calcareous concretions in the north suggest that these deposits are older and more stable. They have changed chemically after they were deposited, but not as much by rivers. When taken as a whole, these maps show that the Cooch Behar Plain is a lowland that is dominated by rivers and is constantly changing geomorphically as a result of channel migration, flooding, and sedimentation. A intricate arrangement of depositional landforms has developed as a result of the interplay between rock types and river processes; ancient deposits preserve the paths of previous river systems, while the ongoing movement of sediments shapes the present landscape. Therefore, the area is a good example of a dynamic floodplain environment, where evolutionary processes of the river and landscape modification are under the influence of both erosional processes and depositional processes.

Five longitudinal elevation profiles (CP-1 to CP-5) are shown plotted against distance (m) in Figure 3, which are most likely to represent different river transects or channel traces. All profiles exhibit a

general increasing downward trend in elevation with increasing distance which indicates that there is a gradual decrease in gradient downstream. A steep trunk with moderate undulations is indicated at CP-1 that begins at about 80-85 m and ends at about 55 m over 40000 m. Greater amplitude oscillations in CP-2, which start at about 65 m and get smaller to about 50 m, are suggestive of unequal channel gradients and potentially small erosional-depositional zones. A transitional intermediate reach with significant variability at 33 km and a steady decline from about 60 to 45 meters is identified by CP-3.

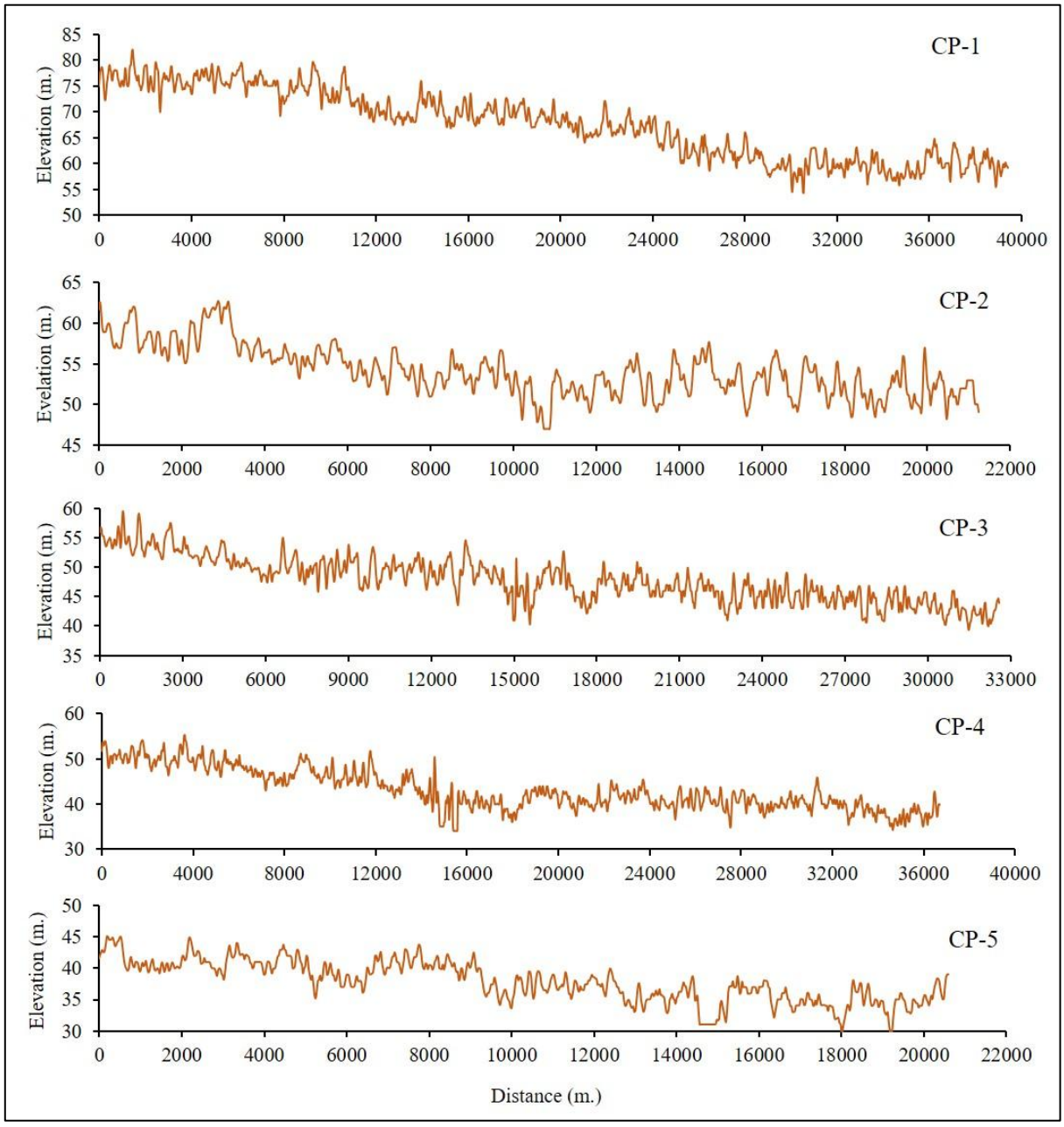

Fig. 3. Floodplain elevation profiles of river Jaldhaka; CP-1, CP-2, CP-3, CP-4, and CP-5 are the cross-sectional profiles on Jaldhaka floodplain in the Cooch Behar plain.

Although there are some oscillations, CP-4 drops steadily from 60 m to about 40 m, which could indicate a more stable region with less variation in relief. Greater amplitude oscillations in CP-2, which start at about 65 m and get smaller to about 50 m, are suggestive of unequal channel gradients

and potentially small erosional-depositional zones. With an elevation range of only 45 to 35 meters over 20,000 meters, CP-5 indicates a depositional lower reach with little slope variation. As a river system transitions from upland to lowland, the profiles generally show a progressive drop in elevation and slope from CP-1 to CP-5. The undulations seen in every profile point to localized geomorphic irregularities brought on by variations in flow velocity, sediment load, and erosion. While smoother patterns in CP-4 and CP-5 suggest sediment accumulation and lower energy, the relatively steep slopes in CP-1 and CP-2 indicate active incision. Together, these patterns show a dynamic fluvial environment that is evolving towards a graded river profile with areas of both active erosion and deposition.

4.2 Channel Oscillation on the Floodplain of Jaldhaka River System

The River Jaldhaka in the Cooch Behar plain exhibits contrasting geomorphological and hydrological characteristics between Window-I and Window-II (Figure 4 – Figure 17). Relict surfaces and previous channel migration are dominant in Window-I, where the older floodplain spans over 450.74 km² and the active floodplain covers 58.63 km². On the other hand, Window-II displays an active floodplain of 80.55 km² and an older floodplain of 81.07 km², indicating a more dynamic and balanced floodplain system. The channel length shows a shift towards a more sinuous channel, increasing from 42.983 km in Window-I to 50.860 km in Window-II. A slight increase in meandering tendencies downstream is confirmed by the Standard Sinuosity Index (SSI), which goes from 1.040 to 1.062.

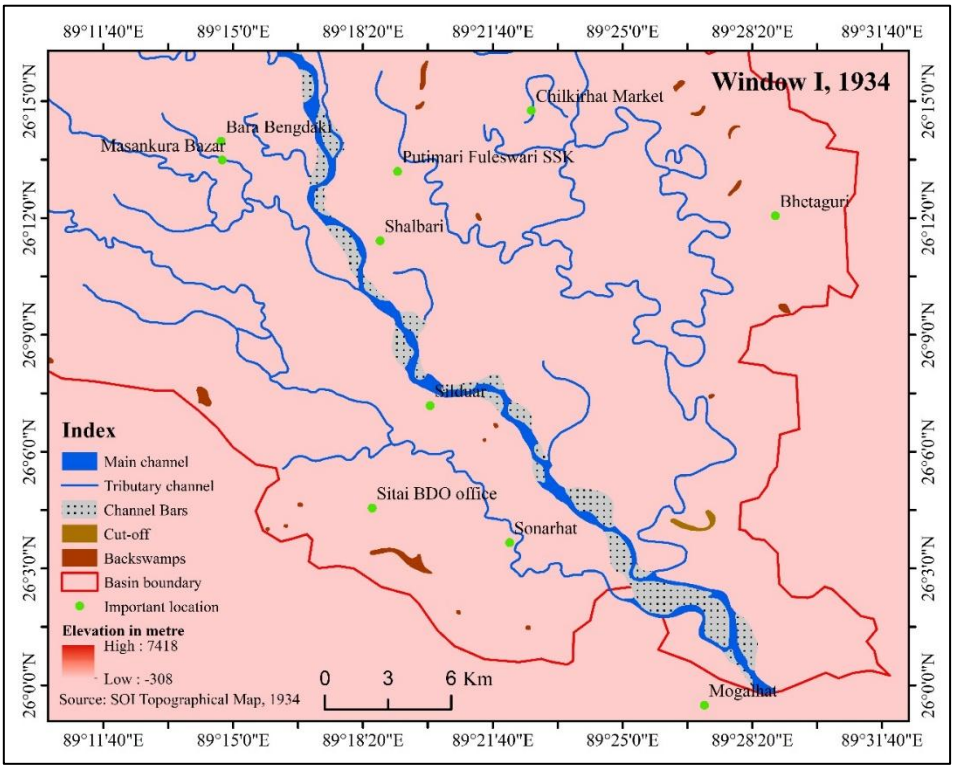

Fig. 4. Floodplain geomorphological settings of the Jaldhaka River in lower Cooch Behar plain in 1934

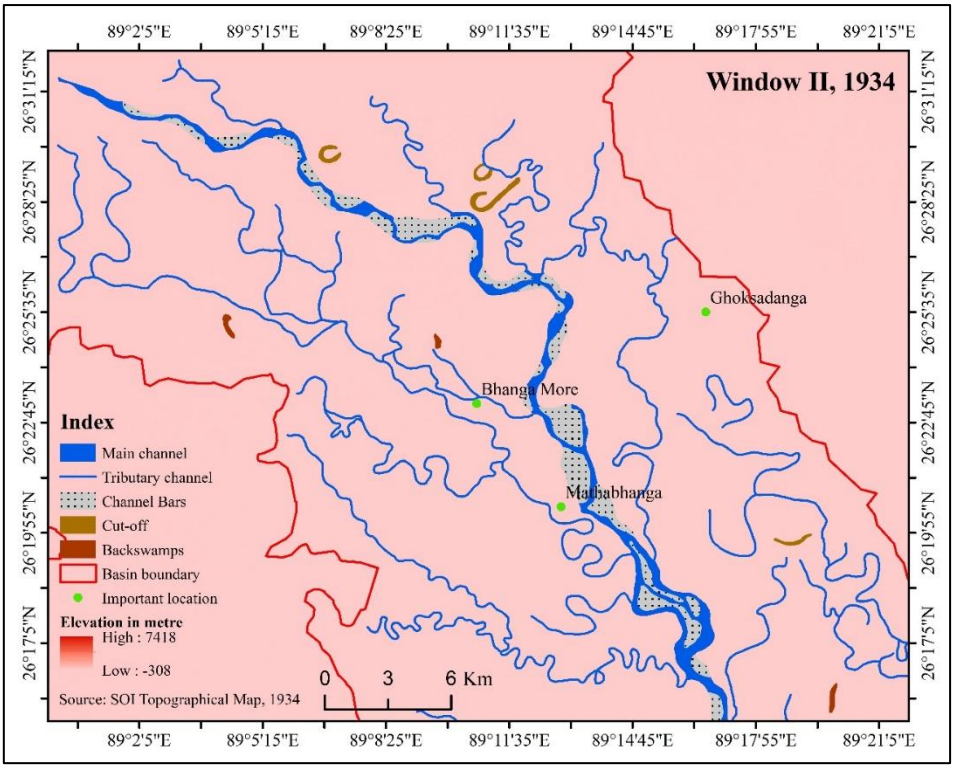

Fig. 5. Floodplain geomorphological settings of the Jaldhaka River in upper Cooch Behar plain in 1934

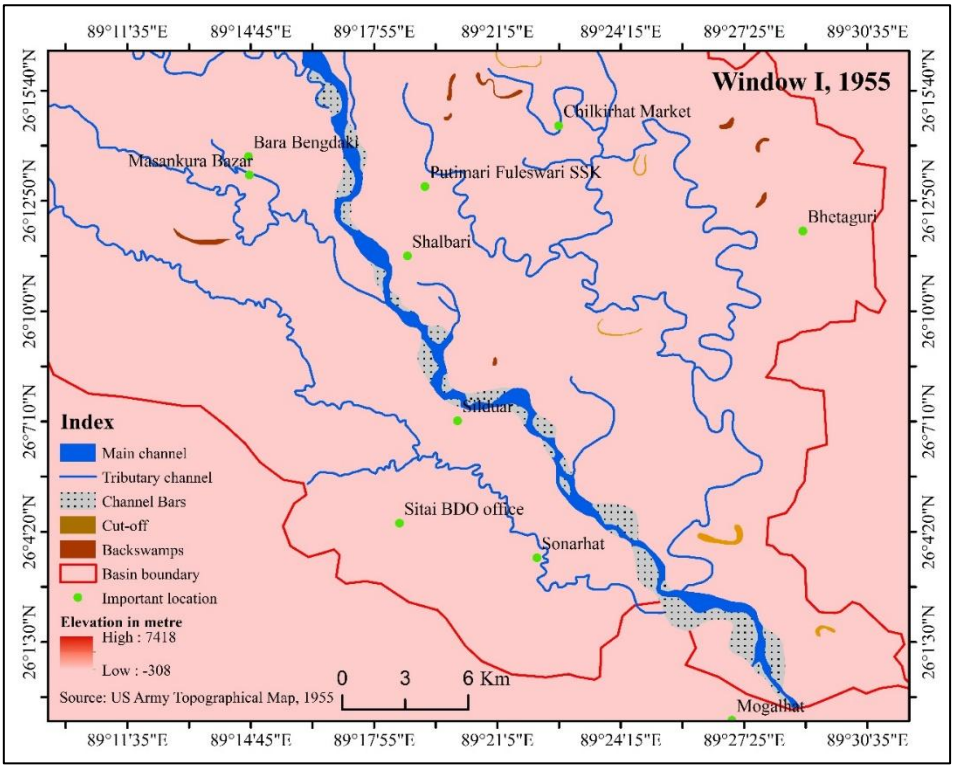

Fig. 6. Floodplain geomorphological settings of the Jaldhaka River in lower Cooch Behar plain in 1955

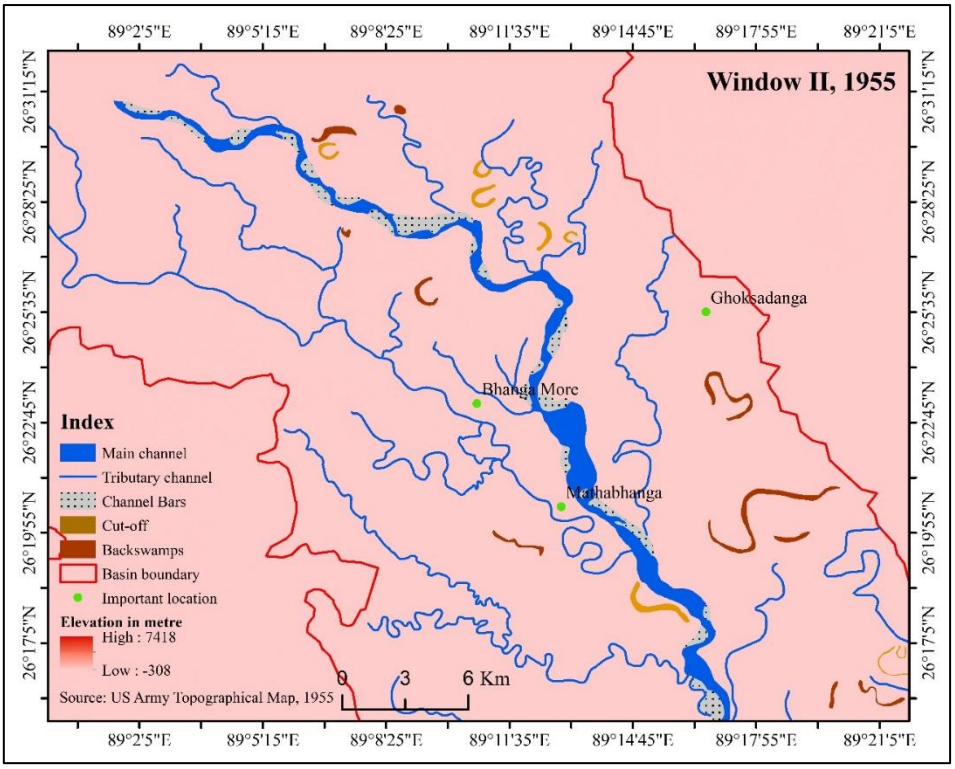

Fig. 7. Floodplain geomorphological settings of the Jaldhaka River in Upper Cooch Behar plain in 1955

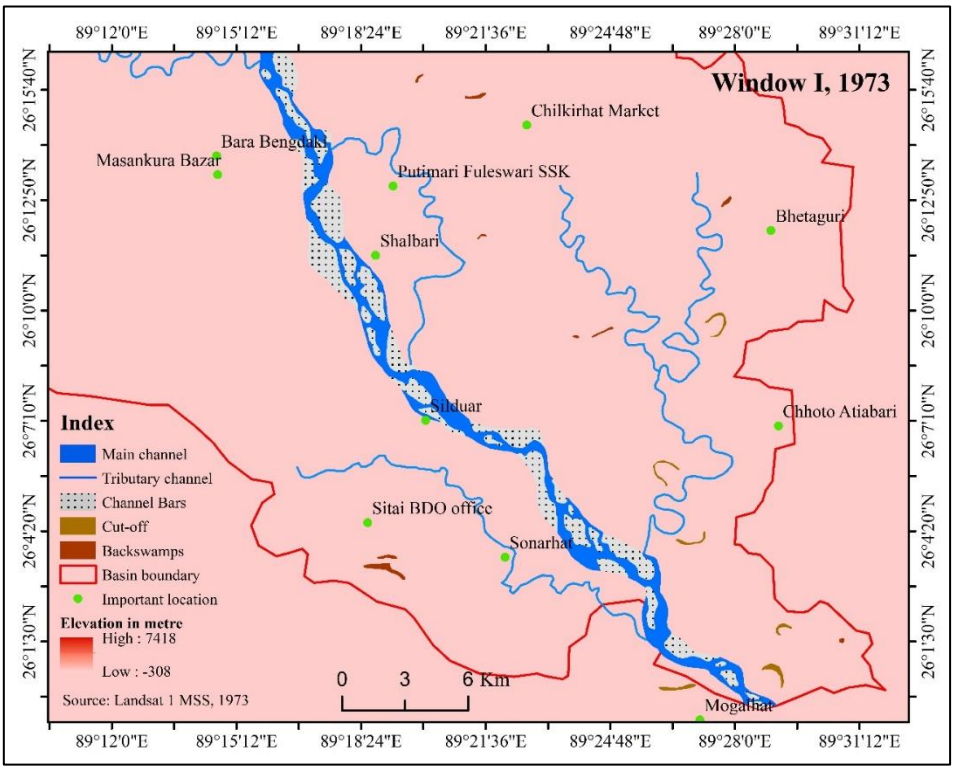

Fig. 8. Floodplain geomorphological settings of the Jaldhaka River in lower Cooch Behar plain in 1973

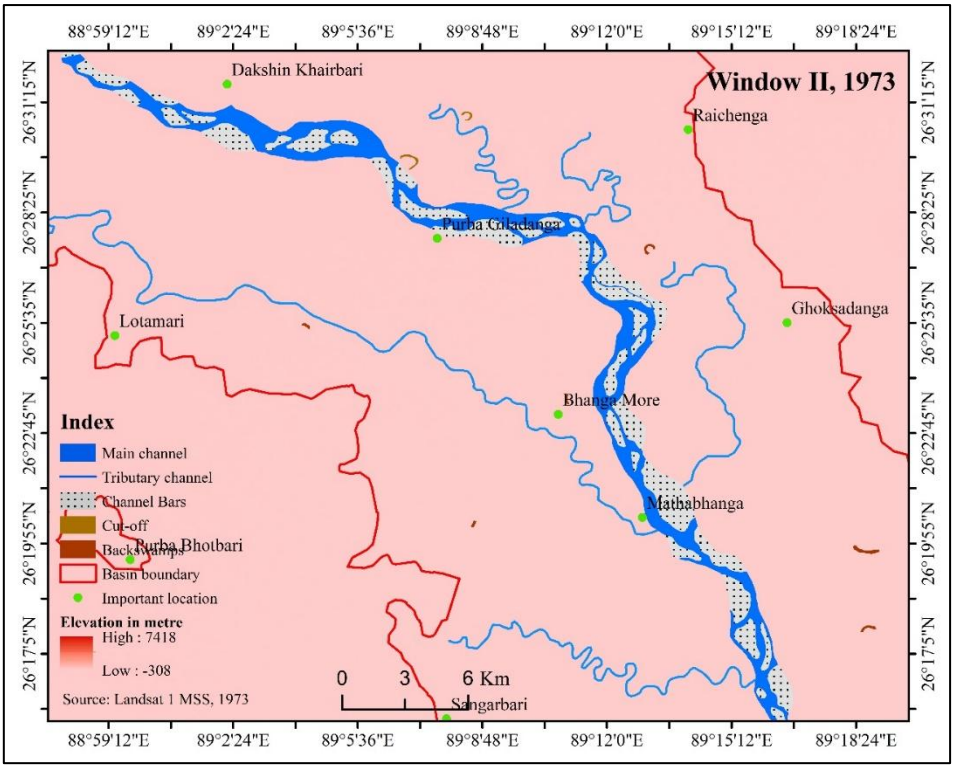

Fig. 9. Floodplain geomorphological settings of the Jaldhaka River in Upper Cooch Behar plain in 1973

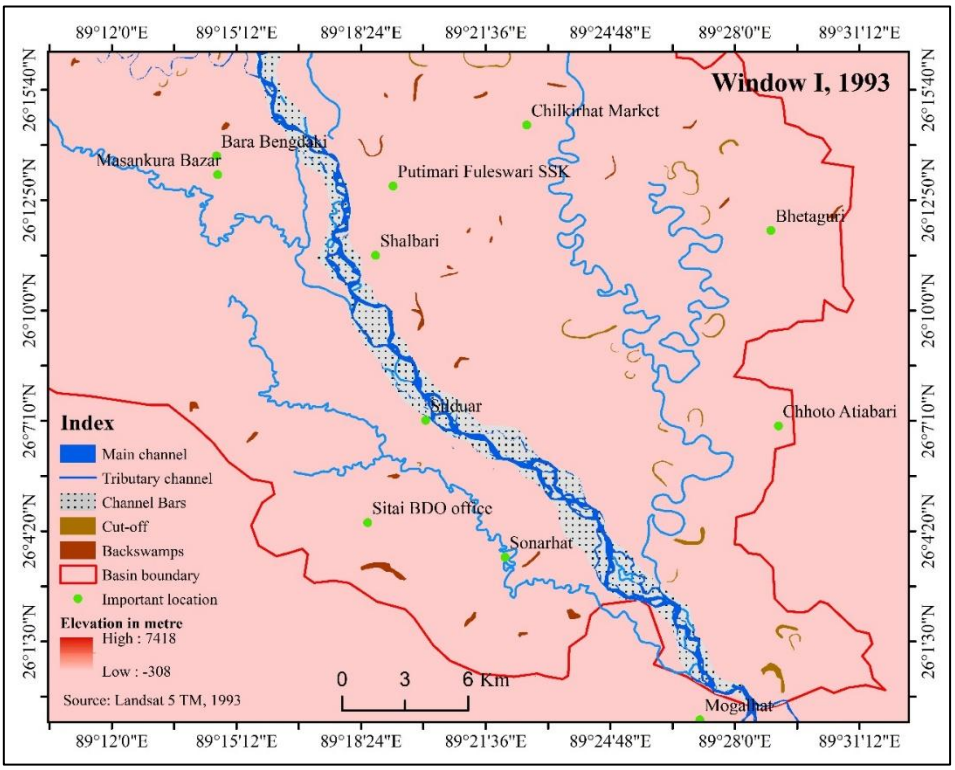

Fig. 10. Floodplain geomorphological settings of the Jaldhaka River in lower Cooch Behar plain in 1993

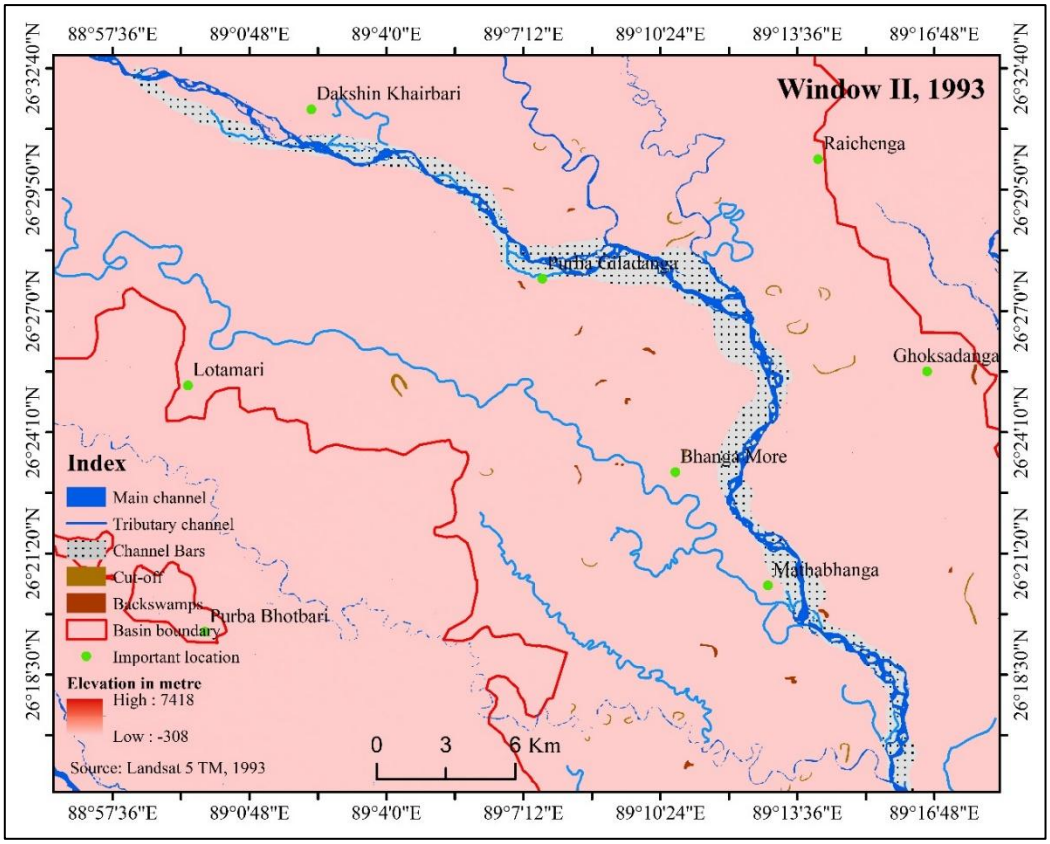

Fig. 11. Floodplain geomorphological settings of the Jaldhaka River in Upper Cooch Behar plain in 1993

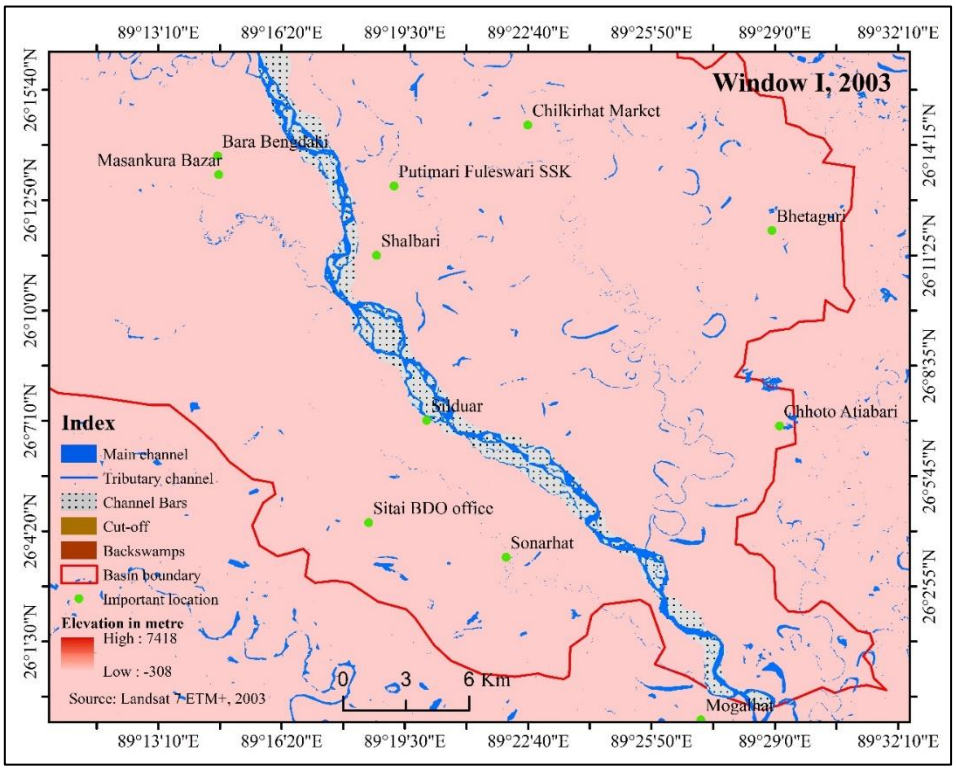

Fig. 12. Floodplain geomorphological settings of the Jaldhaka River in lower Cooch Behar plain in 2003

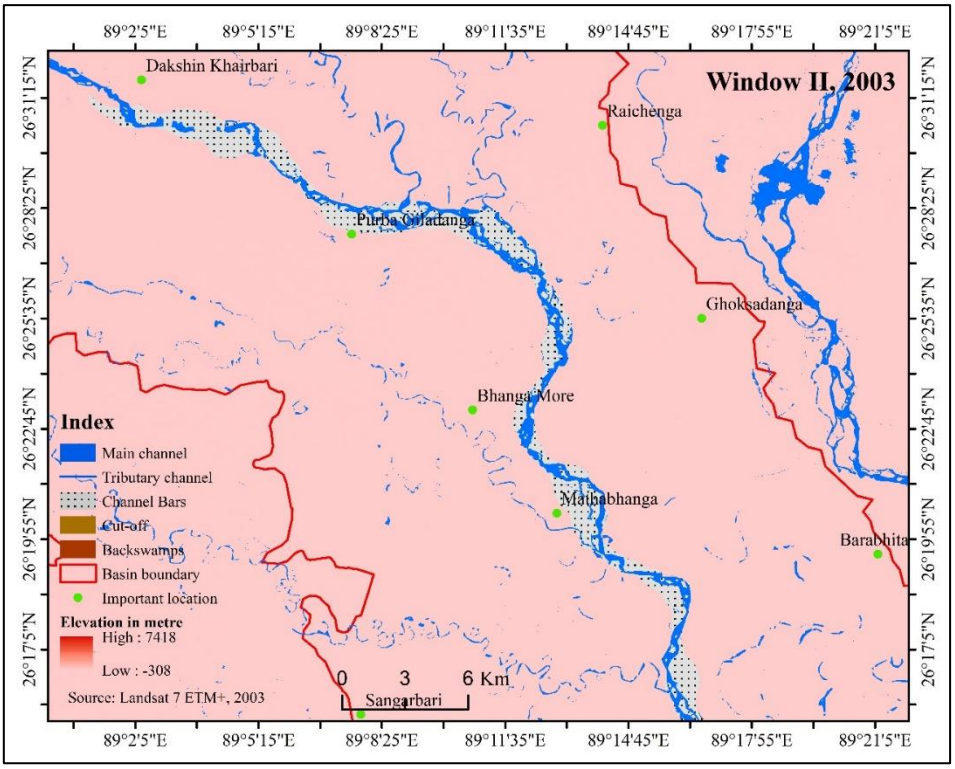

Fig. 13. Floodplain geomorphological settings of the Jaldhaka River in Upper Cooch Behar plain in 2003

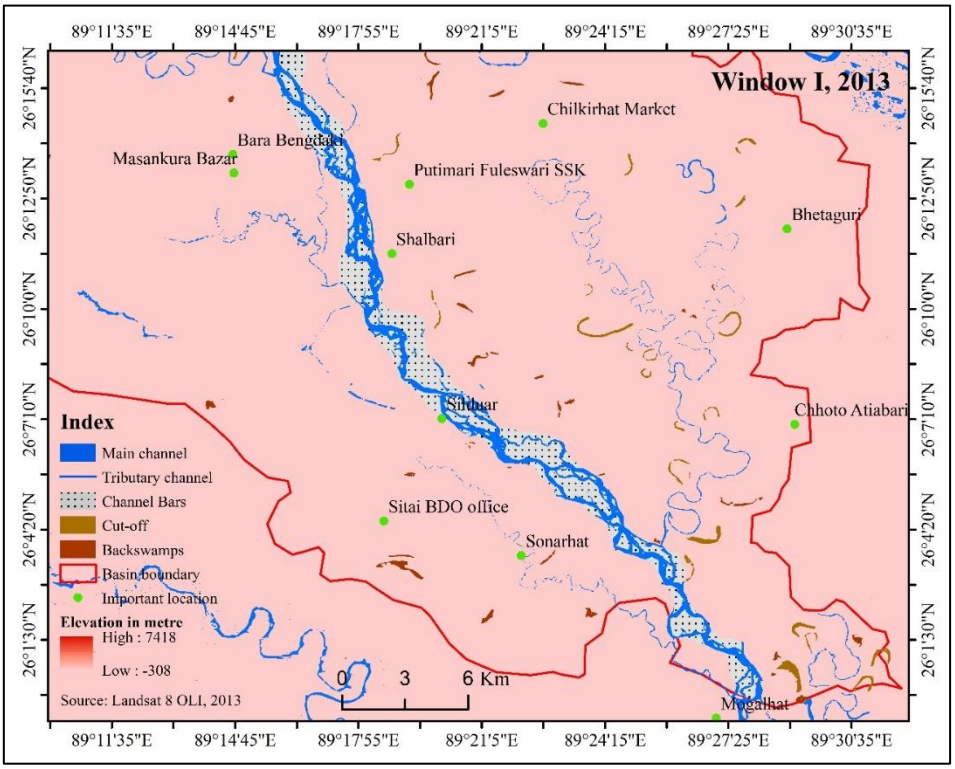

Fig. 14. Floodplain geomorphological settings of the Jaldhaka River in lower Cooch Behar plain in 2013

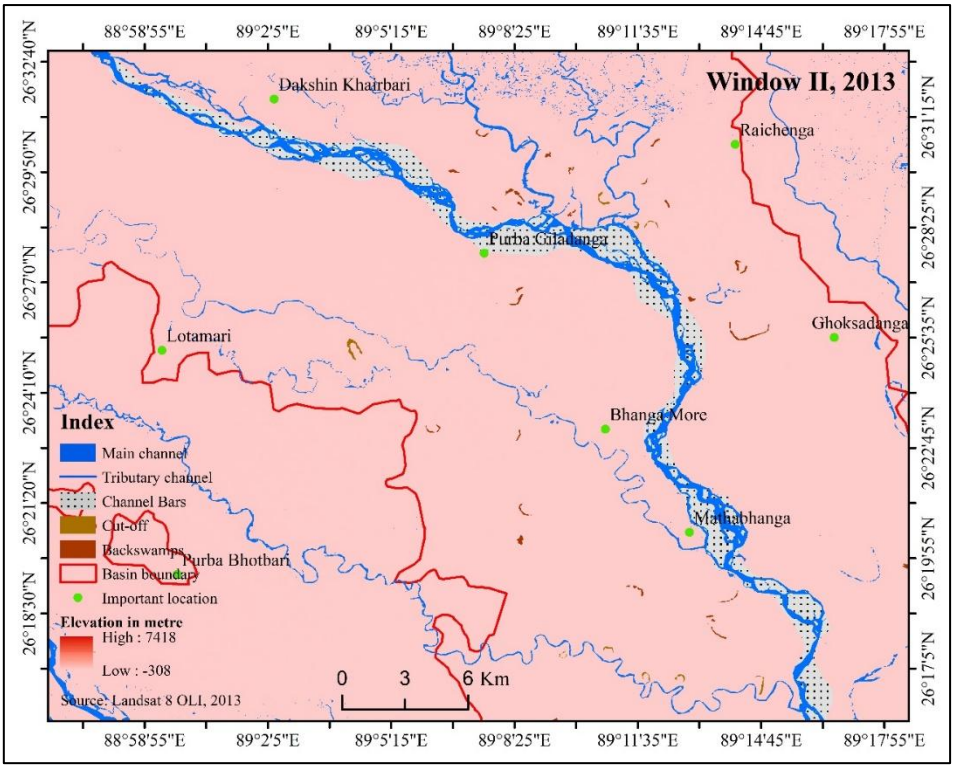

Fig. 15. Floodplain geomorphological settings of the Jaldhaka River in Upper Cooch Behar plain in 2013

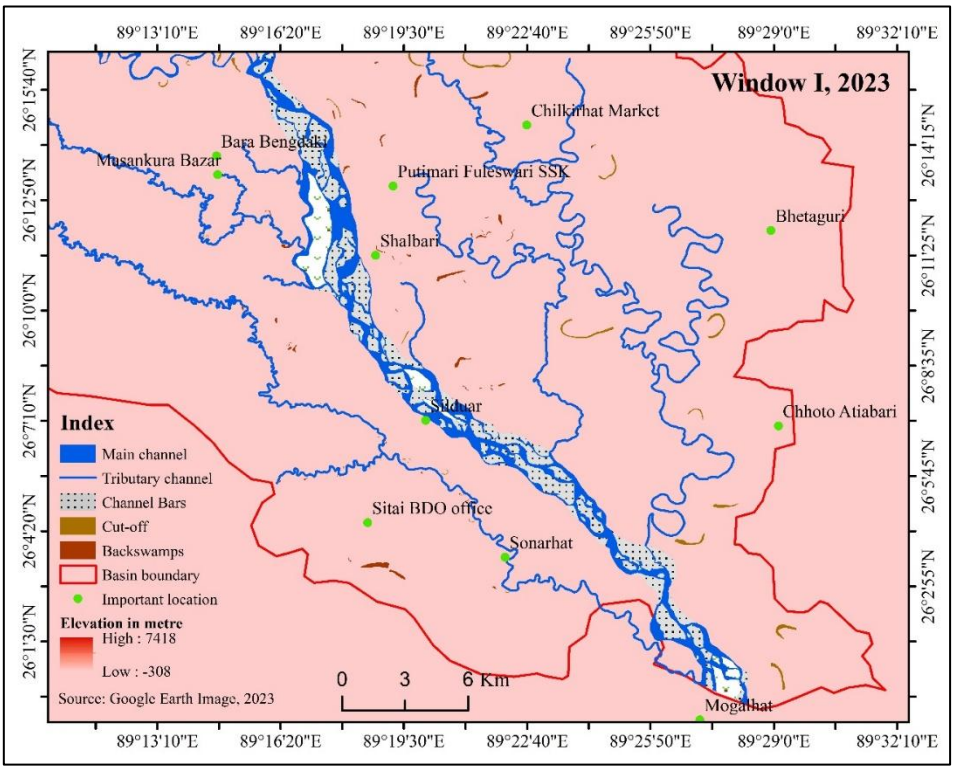

Fig. 16. Floodplain geomorphological settings of the Jaldhaka River in lower Cooch Behar plain in 2023

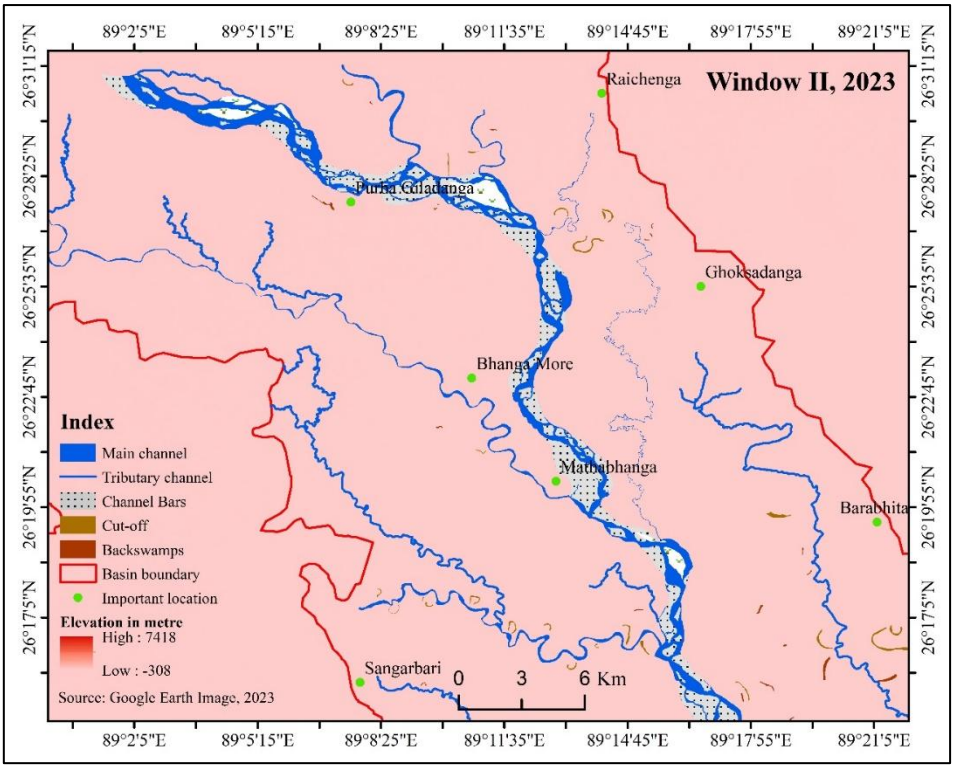

Fig. 17. Floodplain geomorphological settings of the Jaldhaka River in Upper Cooch Behar plain in 2023

Channel sinuosity is increasingly controlled by topography, as evidenced by the Topographic Sinuosity Index (TSI), which rises from 72.050 to 77.865, and the Hydraulic Sinuosity Index (HSI), which falls from 27.950 to 22.135 (Table 1). A shift from a highly braided to a more single-threaded sinuous pattern is indicated by the Braiding Index (BI), which falls from 4.416 to 3.264 (Table 3).

The pattern changes from straight in Window I to sinuous in Window II, although the channel type is alluvial in both windows. Strong sediment transport and sporadic flooding are supported by the average monsoonal discharge, which is still high at 184.839 m^3/s. Both zones exhibit active sedimentation, as evidenced by the main accretion processes of braid channel accretion, overbank vertical accretion, and lateral point bar accretion. Although Window-II also has palaeochannels, which show older flow paths, geomorphological features like oxbow lakes, cut-off meanders, point bars, abandoned channels, and braid bars are common.

Wide variations exist in the floodplain width: Window-I spans 4.821 km to 26.053 km, while Window-II narrows to 1.748–6.871 km, indicating lateral confinement downstream. All things considered, the Jaldhaka River changes from a broad, braided, and older floodplain in Window-I to a smaller, more sinuous, and younger floodplain in Window-II. This shows how a sediment-overloaded braided system downstream gives way to a more stable meandering channel.

Table 1
Displays the hydro-geomorphological features of the River Jaldhaka in the Cooch Behar Plain according to various parameters (channel and floodplain morphology)

Sl. No.	Parameters	Present condition	
		Window-I	Window-II
1	Total floodplain area of river Jaldhaka in the Cooch Behar plain	Active floodplain: 58.63 km^2 Older floodplain: 450.74 km^2	Active floodplain: 80.55 km^2 Older floodplain: 81.07 km^2
2	Channel length in the Cooch Behar plain	42.983 km	50.860 km
3	Standard Sinuosity Index (SSI)	1.040	1.062
4	Topographic Sinuosity index (TSI)	72.050	77.865
5	Hydraulic Sinuosity index (HSI)	27.950	22.135
6	Braiding Index (BI)	4.416	3.264
7	Channel type and pattern	Alluvial channel with straight pattern	Alluvial channel with sinuous pattern
8	Average discharge during monsoon	184.839 m^3/s	
9	Main floodplain accretion process	Lateral point bar accretion, overbank vertical accretion and Braid channel accretion	Lateral point bar accretion, overbank vertical accretion and Braid channel accretion
10	Major floodplain geomorphological characteristics	Oxbow lake, Cut-off meander, point bar, Abandoned channel, meander scar, braid bar, channel island	Oxbow lake, Cut-off meander, point bar, Abandoned channel, meander scar, palaeochannel, braid bar, channel island
11	Maximum floodplain width	26.053 km	6.871 km
12	Minimum floodplain width	4.821 km	1.748 km

Source: Calculated by authors, 2025

Figure 18 shows how the right bank of the Jaldhaka River shifts in space and time across the Cooch Behar plain.

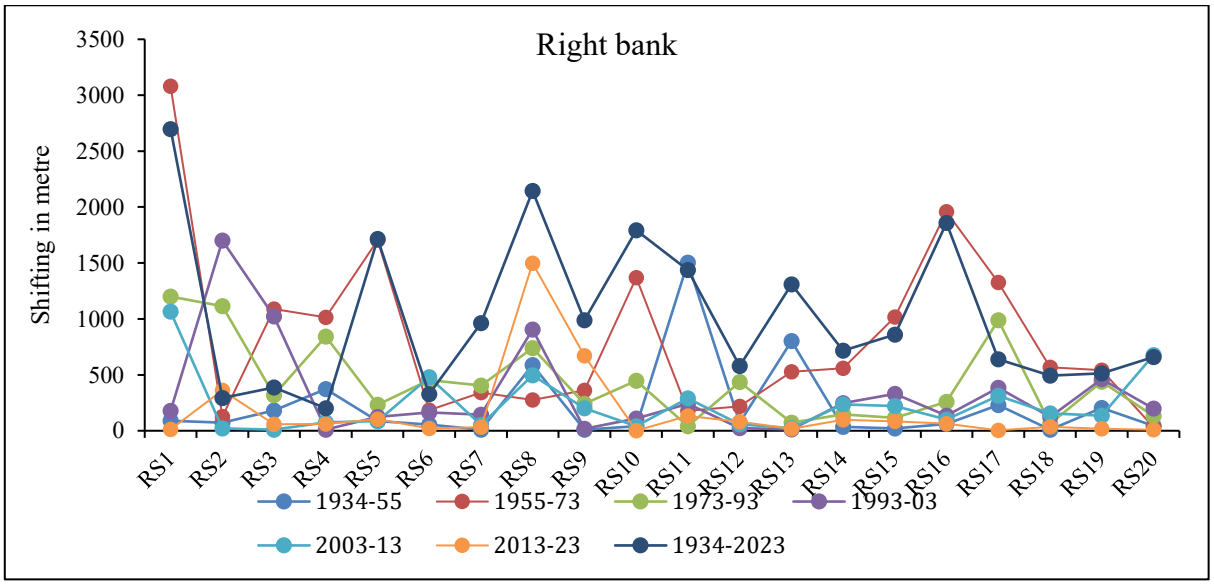

Fig. 18. The Jaldhaka River's right bank line shifts in space and time across the Cooch Behar plain

Figure 19 shows the spatio-temporal shifting of the left bank line of the Jaldhaka River in the Cooch Behar plain.

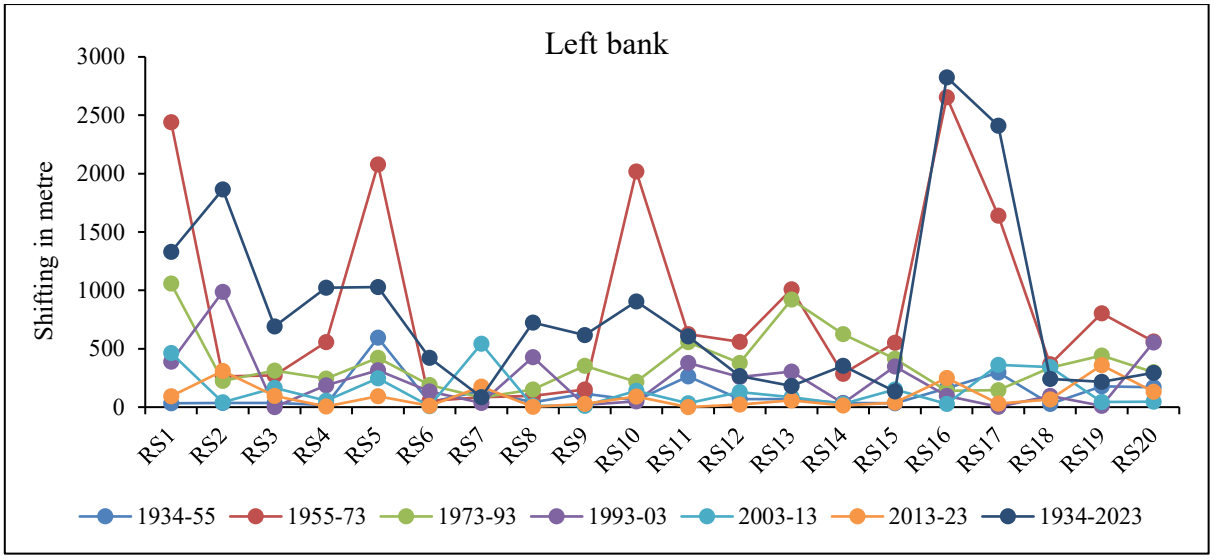

Fig. 19. Spatio-temporal shifting of left bank line of the Jaldhaka River in Cooch Behar plain

The provided dataset, which is separated into two spatial windows (Window-I and Window-II), documents changes in the morphometric and sinuosity of a river channel from 1934 to 2023. The data show clear geographical and temporal variations in air length, valley length, channel length, and inferred sinuosity indices over this 89-year period, indicating fluvial dynamics and geomorphic modifications.

With a channel length of 42.983 km and a valley length of 43.120 km, Window-I produced a channel index of 1.178 and a valley index of 1.182 in 1934. Compared to the hydraulic sinuosity index (HSI), which was -2.104 and indicated slight hydraulic straightening, the topographic sinuosity index (TSI), which was 102.104, indicated a slightly more sinuous topography. With a TSI of 90.678 and a channel index of 1.345, Window-II of the same year displayed somewhat higher sinuosity, emphasizing more noticeable meandering (Table 2).

Table 2
Sinuosity parameter values computed for the various Jaldhaka River segments in the Cooch Behar Plain

Year	Window	CL (km)	VL (km)	AL (km)	CI (km)	VI (km)	TSI	HIS	SSI
1934	Window-I	42.983	43.120	36.473	1.178	1.182	102.104	-2.104	0.997
	Window-II	50.860	49.645	37.827	1.345	1.312	90.678	9.322	1.024
1955	Window-I	43.685	43.146	36.473	1.198	1.183	92.526	7.474	1.012
	Window-II	50.637	49.829	37.827	1.339	1.317	93.692	6.308	1.016
1973	Window-I	42.122	40.634	36.473	1.155	1.114	73.659	26.341	1.037
	Window-II	46.398	46.697	37.827	1.227	1.234	103.489	-3.489	0.994
1993	Window-I	43.653	39.924	36.473	1.197	1.095	48.064	51.936	1.093
	Window-II	48.381	47.274	37.827	1.279	1.250	89.511	10.489	1.023
2003	Window-I	43.723	41.416	36.473	1.199	1.136	68.179	31.821	1.056
	Window-II	49.605	47.554	37.827	1.311	1.257	82.586	17.414	1.043
2013	Window-I	41.951	40.714	36.473	1.150	1.116	77.419	22.581	1.030
	Window-II	48.959	47.721	37.827	1.294	1.262	88.879	11.121	1.026
2023	Window-I	42.337	40.698	36.473	1.161	1.116	72.050	27.950	1.040
	Window-II	51.281	48.303	37.827	1.356	1.277	77.865	22.135	1.062

Source: Computed by authors, 2025

By 1955, Window-I's meanders had slightly stabilized (TSI of 92.526) and its sinuosity had slightly increased (channel index 1.198). Window-II's sinuosity slightly dropped (channel index 1.339) in comparison to 1934, suggesting localized adjustments. The standard sinuosity index (SSI), which remained close to unity in both windows, demonstrated overall planform stability. Window-I's channel length decreased to 42.122 km in 1973 when indices dropped to 1.155 and 1.114, suggesting a possible straightening and a decrease in sinuosity. Its high hydraulic sinuosity (26.341) and TSI value (73.659) indicate dynamic channel reconfiguration. With a nearly equal channel and valley length ratio (TSI 103.489, HSI -3.489), Window-II displayed a brief return to equilibrium. By 1993, the HSI had increased dramatically to 51.936 and the TSI had dropped to 48.064, suggesting a substantial hydraulic reorganization that may have been caused by floods or human activity. Window-II's sinuosity remained modest with a channel index of 1.279 and a balanced TSI of 89.511. In 2003, both windows shown a return to modest stability. Window-I's TSI rose to 68.179, while Window-II's increasing sinuosity (channel index 1.311, SSI 1.043) showed resumed meander growth. This pattern points to a time of recuperation following earlier interruptions. In 2013, Window-I once again displayed reduced sinuosity (channel index 1.150), suggesting further straightening. In contrast, Window-II maintained minor meandering, indicating relative equilibrium, with a TSI of 88.879 and an SSI of 1.026. By 2023, the Window-I indicators (TSI 72.050, channel index 1.161) had recovered in a rather sinuous manner. Window-II, on the other hand, exhibited the highest observed sinuosity (channel index 1.356, SSI 1.062), suggesting higher meander complexity and lateral migration. Overall, the findings indicate that Window-I exhibited more pronounced sinuosity changes, which were most likely brought on by valley constriction and hydrological variability. The greater and more constant sinuosity of Window-II indicates a wider floodplain and more lateral motion. The standard sinuosity index remained close to 1.0 over the time (0.994–1.062), indicating that the overall channel shape remained in a quasi-equilibrium condition despite local modifications. From 1934 to 2023, there is a minor long-term tendency towards increased sinuosity in Window-II and periodic cycles of straightening and recovery in Window-I. The alternating dominance of hydraulic action and structural control is shown in the inverse connections between the topographic and hydraulic sinuosity indices; as one rises, the other tends to plummet. Peaks in HSI values (like 1993 and 2003) most likely correspond with hydrological events or human activity that influences flow energy. For comparison, the constant air length (36.473 km in Window-I; 37.827 km in Window-II) demonstrates that although the channel's shape altered, its geographical expanse did not. Over the course of over 90 years, the fluvial system has shown resilient, adapting to times of widening, re-meandering, and straightening.

Table 3
Values of Braiding index (BI) calculated for the different sections of Jaldhaka River in Cooch Behar Plain

Window	1934	1955	1973	1993	2003	2013	2023
Window-I	2.020	1.922	1.388	3.103	3.353	3.407	4.416
Window-II	1.962	1.296	2.739	3.160	2.975	3.451	3.264

Source: Computed by authors, 2025

The braided index data for Window-I and Window-II from 1934 to 2023 show clear temporal fluctuations in the degree of channel braiding, reflecting changes in river dynamics, sediment load, and flow regime over almost 90 years.

Window-I's braided index of 2.020 in 1934 and Window-II's 1.962 show that both portions had moderate braiding with several interconnecting channels. By 1955, Window-I had dropped to 1.922 and Window-II to 1.296, suggesting a time of channel stabilization or reduced sediment input. In 1973, the pattern changed dramatically: Window-II's braided index dropped to 1.388, indicating channel simplification and the dominance of a single-thread channel, while Window-II's index

increased to 2.739, indicating localized reactivation of braiding, possibly due to increased discharge or sediment deposition. Braiding had significantly recovered to both windows by 1993, with Window I reaching 3.103 and Window II reaching 3.160. This notable alteration points to enhanced river activity, most likely as a result of high-energy hydrological events or channel division brought on by floods. The 2003 braided condition, which indicated channel stability adjustment and uneven sediment redistribution, increased even more in Window-I (3.353) but considerably declined in Window-II (2.975). By 2013, both windows had reached their greatest levels of braiding since 1934, with indices of 3.407 (Window-I) and 3.451 (Window-II), suggesting a highly dynamic river pattern characterised by many bars, islands, and active channel movement. In 2023, Window-I's braided index shot up to 4.416, the highest number ever recorded, indicating extreme channel fragmentation and sediment overload conditions. However, Window-II showed a little decline to 3.264, suggesting either partial stabilization or downstream channel consolidation.

All things considered, the findings indicate a progressive shift to a more unstable, sediment-rich regime, with a long-term rise in braiding intensity, particularly in Window-I. While braiding has also increased in Window-II since 1934, its temporal variability is slightly higher, indicating that channel consolidation and expansion have alternated. Significant geomorphic reorganization is indicated by the sharp rise after 1973, which could be brought on by anthropogenic impacts like deforestation or embankment alteration, climate change, or an increase in the frequency of floods. Before going into a highly braided, dynamic period from 1973 to 2023, the system was relatively steady from 1934 to 1955. This development shows a slow rise in fluvial energy and sediment movement, especially in the narrow portions depicted by Window-I. Rising braided index values are associated with improved lateral movement, more sediment reworking, and higher hydraulic complexity. All things considered, the data demonstrates that the river has become increasingly braided over time, signifying a shift from a semi-stable to a highly dynamic and geomorphically active fluvial system.

5. Discussion

Table 4 presents data on Location, Date, Time, MAGMB, Depth (km), and MW for major earthquakes during the recent period (1990–2020) in and around the Jaldhaka River Basin. The results of the statistical data on the right bank line (Table 5) suggest that there are significant spatial differences in channel behaviour, and that it appears to move across the 20 sites (RS1-RS20). Everything being equalized, there is variation of values in all directions that indicates that the right bank has experienced mild and extreme lateral migration at different points (Fig. 18). The range in RS12 is the lowest (19.34 m), which means that it is relatively stable; however, in RS1, the highest range is 169.78 m, which means a lot of channel instability. The mean shifting values indicate that localized differences in the processes of erosion and deposition exist: the values shift significantly (from 8.60 m at RS12 to 56.30 m at RS8). Much variation in the changing magnitude of shifts is captured in the high values of standard deviation at the sites of RS1 and RS2, and this could have been caused by shifting energy in nearby flow or the sediment load. The coefficient of variation (CV) values are generally above 100 and this means that there is exceptionally irregular movement of channels along most of the sites. There are very unstable shifting patterns in such sites as RS2 (CV = 153.78) and RS20 (CV = 158.48) which can suggest the presence of dynamic and changeable sections. RS7 and RS14, however, exhibit the least CV with value of 74.64 and 72.94 respectively; the shifting trends are relatively homogeneous. There are more dominant events with higher stores, with some extreme deviations, which are reflected in a positive skew at nearly every location. RS5 and RS16 possess the largest skewness (2.54 and 2.52) and thus can be considered hotspots of abrupt and episodic bank migration. The values of kurtosis are positive, as extreme shifting episodes may happen

at any place but favor more locations that are at risk. The fact that there are certain instances of lateral migration albeit very sharp indicates the existence of the highest kurtosis values at RS5 (6.55) and RS16 (6.48). Less active activity and more consistent shifting magnitudes is indicated by negative kurtosis in RS7, RS14 and RS13. The mixture of high kurtosis and high skewness of a few reaches indicates intermittent instability and not a constant migration in the river channel. The changing trend on the right bank, all said and done, depicts a complex interplay between the hydrodynamic and geomorphological factors. The lower (RS7-RS14) reaches are relatively stable but the upper and intermediate (RS1-RS6) reaches are relatively unstable and variable. However, there is a renewed instability, again, at some lower locations (RS16 and RS20); this may be due to anthropogenic factors or constriction of the channel. Everything being what it may, the behaviour of the right bank is extremely dynamic with alternating periods of stability and instability, which is an expression of the variability with which the fluvial processes of the river corridor evolve.

Table 4
Major earthquake during the recent period (1990-2020) in and around Jaldhaka River Basin

Sl. No.	Location	Date	Time	MAGMB	Depth (km)	MW
1	27.0171 N, 88.8378 E	23.05.2012	20:27:28	3.9	17.00	4.345
2	26.7746 N, 89.092 E	12.03.2016	16:15:12	3.9	14.88	4.345
3	26.581 N, 88.9575 E	23.09.2009	02:01:21	3.4	35.00	3.920
4	26.40 N, 89.1399 E	16.01.1994	14:22:39	4.8	33.00	4.800
5	26.2800 N, 89.2200 E	27.05.2004	00:22:15	4.0	10.00	4.430
6	26.33 N, 88.9199 E	29.12.2002	07:05:03	4.8	1.00	4.800
7	26.3129 N, 89.0275 E	30.10.2005	16:23:32	3.1	10.00	3.665
8	26.2933 N, 88.9185 E	25.02.2012	08:45:55	3.7	13.10	4.175
9	26.0259 N, 89.5651 E	22.07.2014	22:58:29	4.2	8.40	4.600
10	26.0549 N, 89.5568 E	11.09.2015	23:56:59	4.0	18.50	4.430
11	26.2364 N, 89.5335 E	22.07.2014	23:35:15	4.0	14.91	4.430
12	26.2701 N, 89.5271 E	13.07.2009	07:39:10	3.3	31.80	3.835
13	27.00 N, 88.9000 E	23.03.1996	16:07:32	3.9	33.00	4.345
14	27.0774 N, 88.9007 E	16.01.2019	23:56:11	3.8	10.00	3.800
15	27.1536 N, 88.6522 E	25.12.2008	00:26:35	4.5	39.40	4.855
16	27.17 N, 88.9599 E	25.05.2003	04:57:04	3.8	5.00	4.260
17	26.90 N, 89.3000 E	11.05.1992	14:43:26	3.9	33.00	4.345
18	26.6892 N, 89.3842 E	11.11.2011	09:57:33	3.9	23.20	4.345

Source: Geological Society of India, Kolkata

Table 5
Descriptive statistics on rate of bank line shifting at right bank of Jaldhaka River

Sites	Range	Mean	Std. Deviation	CV	Skewness	Kurtosis
RS1	169.78	55.89	62.70	112.18	1.22	0.68
RS2	167.86	39.71	61.06	153.78	2.09	4.52
RS3	101.31	28.34	38.48	135.79	1.57	1.48
RS4	55.35	19.03	21.72	114.13	1.14	-0.25
RS5	90.51	23.04	31.92	138.51	2.54	6.55
RS6	45.88	15.08	16.41	108.82	1.59	2.57
RS7	19.74	10.44	7.79	74.64	0.04	-1.85

Table 5
Continued

RS8	134.42	56.30	48.02	85.28	1.53	1.83
RS9	66.57	18.93	22.60	119.35	2.00	4.56
RS10	75.95	19.45	26.46	136.03	2.09	4.70
RS11	69.59	23.72	22.92	96.60	1.85	3.97
RS12	19.34	8.60	6.62	77.04	1.54	2.47
RS13	37.05	13.03	15.12	116.00	1.02	-0.68
RS14	29.27	15.12	11.03	72.94	0.35	-1.75
RS15	55.61	19.48	19.62	100.69	1.30	1.21
RS16	105.92	25.07	37.37	149.05	2.52	6.48
RS17	73.10	30.19	26.14	86.60	0.57	-0.52
RS18	31.14	10.28	10.81	105.14	1.50	2.20
RS19	44.15	18.43	15.51	84.18	0.96	0.30
RS20	66.65	15.14	24.00	158.48	2.29	5.39

Source: Calculated by authors, 2025

Nonetheless, the channel behaviour pattern is variable and dynamic along the river corridor as revealed by line of left bank (Table 6) moving at sites RS1 to RS20. These reaches are quite volatile as the shift values vary greatly (Fig. 19) with the highest lateral displacement recorded in RS16 (144.60 m) and RS1 (134.13 m). Conversely, other places such as RS6 (12.64 m) and RS3 (16.43 m) demonstrate low shifting and hence are relatively constant and not affected by erosional forces. The mean values with the maximum one being RS1 (42.81 m) and the lowest one being RS6 (4.95 m) also have a similar trend implying that the strength of bank migration is not uniform. Although deviations are lower at the RS3 and the RS6, which point to more regular patterns of movement, deviations on the RS10 (39.31 m) and RS16 (51.56 m) are high, which is an indication of very irregular and sporadic shifting behaviour. The coefficient of variation (CV) suggests a great amount of variability and different erosional intensity on the left bank (it normally is more than 100 percent even at a single site) suggesting that the differently eroded areas were RS8 (155.59 percent) and RS16 (156.17 percent). In contrast, RS3 and RS12 have lower CVs (70.61% and 84.62), which means that they have less predictable and uneven reaction of banks. Most locations characterize skewness to be more of a positive value implying that rather large shifting events are more than small ones. The highest skewness is in RS10 (2.59) and RS8 (2.41), where sudden and asymmetric changes in the form of banks due to an intermittent high-energy flow or flood pulsed occur. Negative skew at RS3 and RS11 is suggestive of a trend towards more uniform or moderate shifting with fewer extremes. Values of kurtosis indicate this trend; the strongly negative kurtosis at RS11 (16.49) and RS15 (15.19) indicates flattered distributions and more regular shifting activity whereas high positive values at RS10 (6.80) and RS16 (6.07) indicate peaked distributions and sporadic extreme shifts. In general, the left bank exhibits both stability and instability in alternation which is likely to be caused by the flow energy, the sediment composition and the local geomorphological conditions. The location ranges (RS6RS13) are relatively steady with smaller and more uniform shifts whereas upstream zones (RS1RS5) are moderately to highly unsteady reflecting the active erosion areas. The reemergence of instability in the downstream portion (RS1416 RS20) of the canal, especially in RS16 and RS17 could be attributed to channel constriction or altered flow dynamics. Having areas of the progressive lateral erosion and temporary stability, the left bank is heterogeneous in terms of the qualitative behaviour of its channel. The reason behind the high skew and kurtosis pattern observed at various locations is mainly the extreme hydrological events that take place and the shifting is more cumulative than gradual.

Finally, the dynamic processes on the left bank demonstrate a multifaceted play of the forces of the natural river, where the areas of relative balance and erosion hotspot are the points of spatial differentiation of channel work.

Table 6
Descriptive statistics on rate of bank line shifting at left bank of Jaldhaka River

Sites	Range	Mean	Std. Deviation	CV	Skewness	Kurtosis
RS1	134.13	42.81	45.38	106.01	1.68	3.31
RS2	97.13	26.07	33.58	128.81	2.19	5.11
RS3	16.43	9.49	6.70	70.61	-0.42	-1.65
RS4	30.38	11.48	10.78	93.88	0.92	0.57
RS5	106.01	34.59	36.59	105.79	2.37	5.94
RS6	12.64	4.95	4.79	96.67	1.21	0.30
RS7	53.29	13.13	18.90	143.98	2.26	5.23
RS8	42.31	9.60	14.93	155.59	2.41	6.07
RS9	16.68	6.35	5.68	89.36	1.51	2.60
RS10	109.46	23.42	39.31	167.85	2.59	6.80
RS11	37.77	17.59	15.59	88.63	0.29	-2.13
RS12	28.74	13.91	11.77	84.62	0.41	-1.67
RS13	54.04	21.75	22.37	102.83	0.73	-1.48
RS14	29.70	8.59	11.15	129.82	1.82	2.79
RS15	33.39	15.48	13.89	89.74	0.35	-1.77
RS16	144.60	33.02	51.56	156.17	2.43	6.07
RS17	90.91	25.55	31.71	124.10	1.81	3.52
RS18	32.88	13.12	11.65	88.78	1.00	0.54
RS19	43.41	17.04	17.49	102.68	0.79	-1.20
RS20	52.12	18.65	18.70	100.32	1.56	2.07

Source: Calculated by authors, 2025

6. Conclusion

The geomorphological and lithological assessment of the Cooch Behar Plain during 1934-2023 is that the area is dynamic, and its geologic and physical character are allure by the recurrent flooding, deposition, and continued river movement. The lateral migration and reorganisation of channels can be detected by the presence of levees, oxbow lakes, meander scars and the existence of defunct channels. Lithological patterns of sand, silt, and clay witness to the active processes of alluvial origin and strong interrelation between the texture of sediments and the state of the fluvial energy. The elevation profiles of the sections of the river indicate a change in erosion levels to the upper parts of the river as well as into the lower parts which are characterized by the decreased slope to the downstream.

The Jaldhaka River system has clear spatial and temporal change in terms of channel form whereby, Window-I with a broader, older, and more braided floodplain and Window-II with smaller channel with narrower and meandering form. Adaptation to hydrological and geomorphic changes in the river is manifested by the switching back and forth between situations of straightening, re-meandering, and stabilisation of the channels that can be seen in relation to the sinuosity and braiding indices within the 89 years period. The confinement of the Valley also led to the Window-I having more variation than Window-II that had less lateral movement and more consistent

meandering. A time analysis of the braiding indexes suggests that there had been a gradual growth in the activity of the fluvial after the year 1973, which was perhaps due to the effect of floods, human activities, and global warming. The transition to more hydraulically complex and fluid forceful processes in the river is pointed out by the morphology of the river which shifted to being semi-stable to becoming extremely braided and sinuous. This dynamism is also justified by bank line shifting data, whereby there are areas of instability and stability which are alternating along the two riverbanks. The left bank shows stable areas punctuated with insular erosion hot spots whereas the right bank shows areas of episodic instability in the upper and lower sections. Many of these locations have large skewness and kurtosis values, indicating that the migration of channels is mainly bounded by the extreme hydrological processes, as opposed to the slow processes. Generally, Cooch Behar floodplain is geomorphically active and is constantly being renegotiated as a result of the interaction of both natural fluvial processes and human induced changes. The paper highlights the dynamism and resilience of the Jaldhaka River system whereby channel oscillation, erosion, and deposition interact to keep a rapidly changing topography of floodplain.

Acknowledgements
The Army Map Service (RMBM), U.S. Army Corps of Engineers, provided the U.S. Army Corps of Engineers Series-U502 map, and the authors thank the USGS for providing satellite imagery. We also acknowledge the Central Water Commission, Government of India (CWC, Jalpaiguri), which provided the Jaldhaka River's monsoon season discharge data. The authors also express their sincere gratitude to the Geological Survey of India (GSI) for providing data on the geomorphology and geology of the research region.

Conflicts of Interest
The authors declare no conflicts of interest.

References
[1] Syvitski, J. P., Overeem, I., Brakenridge, G. R., & Hannon, M. (2012). Floods, floodplains, delta plains—a satellite imaging approach. Sedimentary Geology, 267, 1-14. https://doi.org/10.1016/j.sedgeo.2012.05.014
[2] Nanson, G. C., & Croke, J. C. (1992). A genetic classification of floodplains. Geomorphology, 4(6), 459-486. https://doi.org/10.1016/0169-555X(92)90039-Q
[3] Wolman, M. G., & Leopold, L. B. (1957). River flood plains: some observations on their formation (No. 282-C, pp. 87-109). US Government Printing Office.
[4] Maity, S. K., & Maiti, R. (2017). Sedimentation in the Rupnarayan River: Volume 1: Hydrodynamic processes under a tidal system. Springer. https://doi.org/10.1007/978-3-319-62304-7
[5] Clerici, A., Perego, S., Chelli, A., & Tellini, C. (2015). Morphological changes of the floodplain reach of the Taro River (Northern Italy) in the last two centuries. Journal of Hydrology, 527, 1106-1122. https://doi.org/10.1016/j.jhydrol.2015.05.063
[6] Segura-Beltrán, F., & Sanchis-Ibor, C. (2013). Assessment of channel changes in a Mediterranean ephemeral stream since the early twentieth century. The Rambla de Cervera, eastern Spain. Geomorphology, 201, 199-214. https://doi.org/10.1016/j.geomorph.2013.06.021
[7] Shukla, S. S., & Mishra, M. (2019). Tracing of palaeochannels of Bakulahi river system in Uttar Pradesh, India. Arabian Journal of Geosciences, 12(9), 304. https://doi.org/10.1007/s12517-019-4429-6
[8] Rudorff, C. M., Melack, J. M., & Bates, P. D. (2014). Flooding dynamics on the lower Amazon floodplain: 1. Hydraulic controls on water elevation, inundation extent, and river-floodplain discharge. Water Resources Research, 50(1), 619-634. https://doi.org/10.1002/2013WR014091
[9] Trigg, M. A., Bates, P. D., Wilson, M. D., Schumann, G., & Baugh, C. (2012). Floodplain channel morphology and networks of the middle Amazon River. Water Resources Research, 48(10). https://doi.org/10.1029/2012WR011888
[10] Gregory, K. J. (2003). Palaeohydrology, environmental change and river channel management. Palaeohydrology: Understanding Global Change. J. Wiley and Sons, Chichester, 357-378. ISBN 978-0470847398

[11] Srivastava, P., Juyal, N., Singhvi, A. K., Wasson, R. J., & Bateman, M. D. (2001). Luminescence chronology of river adjustment and incision of Quaternary sediments in the alluvial plain of the Sabarmati River, north Gujarat, India. Geomorphology, 36(3-4), 217-229. https://doi.org/10.1016/S0169-555X(00)00058-1
[12] Lauer, J. W., & Parker, G. (2008). Modeling framework for sediment deposition, storage, and evacuation in the floodplain of a meandering river: Theory. Water Resources Research, 44(4). https://doi.org/10.1029/2006WR005528
[13] Erskine, W., McFadden, C., & Bishop, P. (1992). Alluvial cutoffs as indicators of former channel conditions. Earth Surface Processes and Landforms, 17(1), 23-37. https://doi.org/10.1002/esp.3290170103
[14] Toonen WHJ, Kleinhans MG, Cohen KM (2012) Sedimentary architecture of abandoned channel fills. Earth Surf Process Landf 37(4):459–472. https://doi.org/10.1002/esp.3189
[15] Miyazono, S., Aycock, J. N., Miranda, L. E., & Tietjen, T. E. (2010). Assemblage patterns of fish functional groups relative to habitat connectivity and conditions in floodplain lakes. Ecology of Freshwater Fish, 19(4), 578-585. https://doi.org/10.1111/j.1600-0633.2010.00438.x
[16] Zeug, S. C., & Winemiller, K. O. (2008). Relationships between hydrology, spatial heterogeneity, and fish recruitment dynamics in a temperate floodplain river. River Research and Applications, 24(1), 90-102. https://doi.org/10.1002/rra.1061
[17] Asselman, N. E., Middelkoop, H., & Van Dijk, P. M. (2003). The impact of changes in climate and land use on soil erosion, transport and deposition of suspended sediment in the River Rhine. Hydrological Processes, 17(16), 3225-3244. https://doi.org/10.1002/hyp.1384
[18] Ghosh, S., Bera, S., Singh, A., Basu, S., & Basu, R. N. (2022). Hierarchical Bi2WO6/BiFeWO6 nn heterojunction as an efficient photocatalyst for water splitting under visible light. Journal of Alloys and Compounds, 919, 165700. https://doi.org/10.1016/j.jallcom.2022.165700
[19] Graf, W. L. (2006). Downstream hydrologic and geomorphic effects of large dams on American rivers. Geomorphology, 79(3-4), 336-360. https://doi.org/10.1016/j.geomorph.2006.06.022
[20] Brown, T. (2002). Floodplain landscapes and archaeology: fluvial events and human agency. Journal of Wetland Archaeology, 2(1), 89-104. https://doi.org/10.1179/jwa.2002.2.1.89
[21] Chakrabarti, P. (2021). Changing courses of Eastern Himalayan rivers: Flood hazard and irrigation aspects and linking of Brahmaputra–Ganga rivers. Geological Society of India. https://doi.org/10.17491/cgsi/2021/165854
[22] Powers, P. M., Lillie, R. J., & Yeats, R. S. (1998). Structure and shortening of the Kangra and Dehra Dun reentrants, sub-Himalaya, India. Geological Society of America Bulletin, 110(8), 1010-1027. https://doi.org/10.1130/0016-7606(1998)110<1010:SASOTK>2.3.CO;2
[23] Mackey, S. D., & Bridge, J. S. (1995). Three-dimensional model of alluvial stratigraphy; theory and applications. Journal of Sedimentary Research, 65(1b), 7-31. https://doi.org/10.1306/D42681D5-2B26-11D7-8648000102C1865D
[24] Bishop, M. P., & Shroder Jr, J. F. (2004). GIScience and mountain geomorphology: Overview, feedbacks, and research directions. Geographic Information Science and Mountain Geomorphology. Springer-Praxis, New York, 1-31. ISBN 354042640X
[25] Majumdar, B. (2003). Landform and landuse of the Jaldhaka Basin (Doctoral dissertation).
[26] Khawar, G. (2014). Problems of elderly population in Jaldhaka River Basin (Darjeeling District) - a case study (Doctoral dissertation).
[27] Chakraborty, S. (2017). Dynamics of hydro-geomorphological environment in Jaldhaka river Basin of West Bengal and its impact on landuse (Doctoral dissertation).
[28] Rudra, K. (2018). Rivers of the Tarai–Doors and Barind Tract. Rivers of the Ganga-Brahmaputra-Meghna Delta, 27–47. https://doi.org/10.1007/978-3-319-76544-0_3
[29] Chakraborty, S., & Datta, K. (2013). Causes and consequences of channel changes–a spatio-temporal analysis using remote sensing and GIS—Jaldhaka-Diana River System (Lower Course), Jalpaiguri (Duars), West Bengal, India. Journal of Geography and Natural Disasters, 3(1), 1-13. https://dx.doi.org/10.4172/2167-0587.1000107
[30] Mujabar, P. S., & Chandrasekar, N. (2013). Shoreline change analysis along the coast between Kanyakumari and Tuticorin of India using remote sensing and GIS. Arabian Journal of Geosciences, 6(3), 647-664. https://doi.org/10.1007/s12517-011-0394-4
[31] Bhatta, B. (2011). Remote Sensing and GIS (Second Edition). Oxford University press. ISBN 9780198072393
[32] Lillesand, T. M., Kiefer, R. W., & Chipman, J. W. (2015). Remote Sensing and Image Interpretation (7th Edition). Wiley. ISBN 978-1-118-34328-9
[33] Reddy, M. A. (2008). Remote sensing and Geographical Information System (Third Edition). BSP, 1-453. ISBN 978-81-7800-135-7

[34] Mukherjee, R., Bilas, R., Biswas, S. S., & Pal, R. (2017). Bank erosion and accretion dynamics explored by GIS techniques in lower Ramganga river, Western Uttar Pradesh, India. Spatial Information Research, 25(1), 23-38. https://doi.org/10.1007/s41324-016-0074-2

[35] Xu, H. (2006). Modification of normalised difference water index (NDWI) to enhance open water features in remotely sensed imagery. International journal of remote sensing, 27(14), 3025-3033. https://doi.org/10.1080/01431160600589179

[36] Aswathy, M. V., Vijith, H., & Satheesh, R. (2008). Factors influencing the sinuosity of Pannagon River, Kottayam, Kerala, India: An assessment using remote sensing and GIS. Environmental monitoring and assessment, 138(1-3), 173-180. https://doi.org/10.1007/s10661-007-9755-6

[37] Kumar, B. A., Gopinath, G., & Chandran, M. S. (2014). River sinuosity in a humid tropical river basin, south west coast of India. Arabian Journal of Geosciences, 7(5), 1763-1772. https://doi.org/10.1007/s12517-013-0864-y

[38] Brice, J. C. (1964). Channel patterns and terraces of the Loup Rivers in Nebraska. US Government Printing Office. https://doi.org/10.3133/pp422D

[39] Williams, G. P. (1986). River meanders and channel size. Journal of hydrology, 88(1-2), 147-164. https://doi.org/10.1016/0022-1694(86)90202-7

[40] Mueller, J. E. (1968). An introduction to the hydraulic and topographic sinuosity indexes. Annals of the association of American geographers, 58(2), 371-385. https://doi.org/10.1111/j.1467-8306.1968.tb00650.x